Mechanics of Materials 107 (2017) 71–80

Contents lists available at ScienceDirect

Mechanics of Materials

journal homepage: www.elsevier.com/locate/mechmat

Research paper

Nonlinear large deformation of acoustomechanical soft materials

Fengxian Xin[a,b,*], Tian Jian Lu[a,b]

[a] MOE Key Laboratory for Multifunctional Materials and Structures, Xi'an Jiaotong University, Xi'an 710049, PR China
[b] State Key Laboratory for Strength and Vibration of Mechanical Structures, Xi'an Jiaotong University, Xi'an 710049, PR China

ARTICLE INFO

Article history:
Received 12 July 2016
Revised 17 December 2016
Available online 6 February 2017

ABSTRACT

An acoustomechanical theory of soft materials is proposed to account for the nonlinear large deformation of soft materials triggered by both the ultrasound waves and mechanical forces. This theory is formulated by employing the nonlinear elasticity theory of the soft material and the theory of acoustic radiation force, which takes into consideration of the combination loading of mechanical forces and acoustic inputs. While the propagation of acoustic wave depends on material configuration, the radiation force generated by wave propagation deforms the material configuration. This complex interaction reaches a steady state when the mechanical stress and the acoustic radiation stress are able to balance with the elastic deformation stress. The acoustomechanical theory is employed to characterize the acoustomechanical behaviors of thin soft material layers under different boundary conditions (e.g., equal-biaxial forces, uniaxial force, and uniaxial constraint). Prestretches arising from these boundary conditions are shown to play significant roles in affecting the acoustomechanical repsonse of soft material: the same material actuated from different prestretches and boundary conditions exhibits different stretch-stress relations. This novel functionality enables innovative design of acoustic sensors and actuators based on soft materials.

1. Introduction

Soft active materials capable of undergoing large deformation in response to various external stimuli are promising candidates for designing innovative sensors, actuators, medical devices, microfluidic manipulation devices, energy harvesters and adaptive robotics (Stark and Garton, 1955; Zhang et al., 1998; Zhang et al., 2002). A large body of existing works have been devoted to investigating the nonlinear large deformation and instabilities of soft active materials, including dielectric elastomer actuated by electric field (Suo et al., 2008; Zhao and Wang, 2014), magneto-active elastomers trigged by magnitude field (Bustamante et al., 2006; Dorfmann and Ogden, 2004; Rudykh and Bertoldi, 2013), and those sensitive to temperature (Chester and Anand, 2011) and environment salinity (Ohmine and Tanaka, 1982; Tanaka et al., 1980; Yeh and Alexeev, 2015). In sharp contrast, the acoustomechanical actuation performance of soft active materials received much less attention. To address this deficiency, we develop an acoustomechanical theory for the nonlinear deformation of soft materials subjected to combined mechanical force and acoustic inputs. A variety of displacement/force boundary conditions are considered, including equal-biaxial forces, uniaxial force, and uniaxial constraint.

The propagation of ultrasonic wave with a frequency beyond 1 MHz in medium can give rise to a steady time-averaged force called the acoustic radiation force, due mainly to acoustic momentum transfer between adjacent medium particles. This force can reach a magnitude of several times MPa in air when the amplitude of input sound pressure is ~1 MPa, which is sufficient large to induce large nonlinear deformation in common soft active materials with a modulus of several times kPa (Guo et al., 2016; Issenmann et al., 2008; Xin and Lu, 2016a).

Lord Rayleigh first formulated a theory of radiation pressure induced by compressional acoustic waves (Rayleigh, 1902, 1905), while Brillouin was apparently the first to point out the second-rank tensor nature of radiation pressure (Beyer, 1978; Brillouin, 1925). Subsequently, acoustic radiation force has been extensively studied for calculating the acoustic radiation pressure on spheres in the pathway of wave propagation (Doinikov, 1994; Hasegawa and Yosioka, 1969; King, 1934; Yosioka and Kawasima, 1955), for developing acoustical trapping and tweezers (Caleap and Drinkwater, 2014; Evander and Nilsson, 2012; Hu et al., 2007; Marx, 2015; Shi et al., 2009; Silva and Baggio, 2015), for achieving acoustic levitation and contactless handling of matter (Brandt, 2001; Foresti et al., 2013; Foresti and Poulikakos, 2014; Xie et al., 2002), for deforming fluid interface and biological tissue (Issenmann et al., 2008; Mishra et al., 2014; Walker, 1999), for disrupting cross-linked hydrogels for drug release (Huebsch et al., 2014), and so on. These

* Corresponding author.
E-mail addresses: fengxian.xin@gmail.com (F. Xin), tjlu@mail.xjtu.edu.cn (T.J. Lu).

http://dx.doi.org/10.1016/j.mechmat.2017.02.001
0167-6636/

investigations all take advantage of the large magnitude and non-contact merits of acoustic radiation force.

Although the concept of acoustic radiation force has been explored in a variety of practical applications, at present there lacks a comprehensive theoretical model to describe the large nonlinear deformation of soft materials induced by a combination of acoustic radiation forces and mechanical forces in the framework of continuum mechanics. The aim of this study is to formulate such an acoustomechanical theory. To capture the main idea, we consider a thin layer of nearly incompressible soft material subjected to combined mechanical forces and acoustic inputs. Two opposing acoustic waves having identical frequency and amplitude are considered, so that the layer deforms but remains unmoved. The acoustic radiation force is calculated by determining the acoustic fields in and out of the thin material layer (surrounded by fluid), with the nonlinear elasticity of the material accounted for by adopting the Helmholtz free energy function. For illustration, the proposed acoustomechanical theory is employed to analyze three specific cases (equal-biaxial force, uniaxial force, and uniaxial constraint), with special focus placed upon the effects of prestretches caused by different boundary conditions on the acoustomechanical response of the soft material.

2. Acoustomechanical theory of soft materials

Wave propagation in medium is essentially the transport of energy density flux or momentum density flux, which gives rise to radiation stresses in the medium when the propagation occurs at nonlinear level or encounters discontinuous interfaces. For instance, the forces induced by optical wave propagation are referred to as Maxwell electromagnetic radiation stresses and those induced by acoustic wave propagation are called acoustic radiation stresses. In particular, ultrasound wave propagating in soft materials with a frequency as high as 1 MHz is able to generate a steady time-averaged radiation force and hence cause material deformation, since the period of ultrasound wave is too short for material response. This is the case considered in the present study.

Consider a homogenous isotropic soft material, whose bulk modulus $K = E/3(1-2\nu)$ is generally much larger than its shear modulus $G = E/2(1+\nu)$ so that the material is nearly incompressible. As a result, the wave field in the soft material induced by normally incident acoustic waves is dominated by longitudinal waves. In other words, as a good approximation, the nearly incompressible soft material may be taken as fluid-like for wave propagation. Correspondingly, acoustic radiation stress in the medium can be derived by employing the second-order perturbation theory of the Navier–Stokes equation, as (Borgnis, 1953; Lee and Wang, 1993; Livett et al., 1981; Xin and Lu, 2016b,c,d,e):

$$\langle \mathbf{T} \rangle = \left[\frac{\rho_a}{2c_a^2} \left\langle \left(\frac{\partial \phi}{\partial t} \right)^2 \right\rangle - \frac{\rho_a \langle (\nabla \phi)^2 \rangle}{2} \right] \mathbf{I} + \rho_a \langle \nabla \phi \otimes \nabla \phi \rangle \tag{1}$$

where $\langle \mathbf{T} \rangle$ is the second-rank acoustic radiation pressure (stress) tensor, representing compression when positive and tension when negative, $\langle \cdot \rangle$ denotes time-average over an oscillation cycle, $\mathbf{I}$ is the identity tensor, ϕ is the velocity potential, ρ_a is the medium density, and $c_a = (\partial p/\partial \rho)_s$ is the acoustic speed in the medium. Wave propagation in the medium is governed by the Helmholtz equation $\Delta\phi - \frac{1}{c_a^2}\frac{\partial^2 \phi}{\partial t^2} = 0$, which can be solved by combining the corresponding boundary conditions in the Eulerian coordinates. Once the wave field is determined, the acoustic radiation stresses in and out of the material are calculated as:

$$\langle \mathbf{T}^{out} \rangle = \left[\frac{\rho_1}{2c_1^2} \left\langle \left(\frac{\partial \phi_1}{\partial t} \right)^2 \right\rangle - \frac{\rho_1 \langle (\nabla \phi_1)^2 \rangle}{2} \right] \mathbf{I} + \rho_1 \langle \nabla \phi_1 \otimes \nabla \phi_1 \rangle \tag{2}$$

$$\langle \mathbf{T}^{in} \rangle = \left[\frac{\rho_2}{2c_2^2} \left\langle \left(\frac{\partial \phi_2}{\partial t} \right)^2 \right\rangle - \frac{\rho_2 \langle (\nabla \phi_2)^2 \rangle}{2} \right] \mathbf{I} + \rho_2 \langle \nabla \phi_2 \otimes \nabla \phi_2 \rangle \tag{3}$$

where the subscripts "1,2" represent the outside and inside medium, respectively.

The radiation stress falls into the category of field concept as it is induced by acoustic field, which can be treated as part of the material law in Eulerian coordinates. To formulate the acoustomechanical theory, consider next the nonlinear elasticity of soft materials. To this end, the continuum material at a particular time is assigned to the reference configuration. One can thence mark each material particle using its coordinate $\mathbf{X}$ in the reference configuration and mark each spatial point using its coordinate $\boldsymbol{x}$ in the current configuration. Subsequently, the reference configuration $\mathbf{X}$ is mapped to the current configuration $\boldsymbol{x}$ using the deformation gradient $\mathbf{F} = \partial \boldsymbol{x}/\partial \mathbf{X}$. The Cauchy stress is related to the first Piola-Kirchhoff stress via $\sigma = \mathbf{s} \cdot \mathbf{F}^{\mathbf{T}}/\det(\mathbf{F})$. Let $dV(\boldsymbol{x})$ be a volume element with mass density $\rho(\boldsymbol{x})$ and body force $\mathbf{f}^b(\boldsymbol{x}, t)$. Let $\mathbf{n}(\boldsymbol{x})dA(\boldsymbol{x})$ be a surface element with surface force $\mathbf{f}^s(\boldsymbol{x}, t)$, where $dA(\boldsymbol{x})$ is the area of the element and $\mathbf{n}(\boldsymbol{x})$ is the unit vector normal to the interface between two media (e.g., a thin soft material layer and the surrounding fluid; Fig. 1) pointing outside the soft material. Force balance of the volume element is described by $\partial\sigma/\partial \mathbf{x} + \mathbf{f}^b = \rho \partial^2 \mathbf{u}/\partial t^2$, with force boundary condition $\sigma \cdot \mathbf{n} = \mathbf{f}^s$, $\mathbf{u}(\boldsymbol{x}, t)$ being the displacement field.

To be specific, with reference to Fig. 1, consider a thin layer of soft material subjected to combined mechanical force and acoustic inputs. It is assumed that the two opposing incident acoustic waves are time-harmonic plane waves having identical amplitude and frequency, which propagate along the thickness direction of the layer. It is further assumed that the thin soft material layer has a thickness comparable to acoustic wavelength and its in-plane dimensions are much larger. For instance, a layer of dimensions 5 mm × 100 mm × 100 mm satisfies this condition if an incident ultrasound wave traveling with a frequency on the order of MHz is of concern. The thin layer with initial undeformed dimensions (L_1, L_2, L_3) in the reference configuration is deformed to dimensions (l_1, l_2, l_3) in the current configuration. For the problem shown schematically in Fig. 1, the acoustomechanical theory can be formulated by incorporating the acoustic stress field into the nonlinear elastic stress field, so that the soft material behaves as an acoustomechanical responsive material to external mechanical forces. Consequently, its constitutive law can be rewritten as:

$$\sigma_{ij} = F_{iK} \frac{\partial W(\mathbf{F})}{\partial F_{jK}} - \langle T_{ij} \rangle - p_h \delta_{ij} \tag{4}$$

where $W(\mathbf{F})$ is the Helmholtz free energy, which is a symmetric function of the principal stretches (λ_1, λ_2, λ_3) for an isotropic soft material, and p_h is the Lagrange multiplier to ensure the constraint of nearly incompressibility ($\lambda_1\lambda_2\lambda_3 \approx 1$), which pertains to the hydrostatic pressure. Note that the acoustic radiation stress is put on the right side of Eq. (4), implying that the acoustic input is considered as an insider, i.e., the acoustic radiation stress behaves as part of the material law since it is a field force. When a focused ultrasound wave with high intensity is incident upon the soft material, the induced acoustic radiation stress $\langle T_{ij} \rangle$ can be comparable with mechanical stress, thus enabling large nonlinear deformation to develop in the material.

In the Cartesian coordinates of Fig. 1, the acoustic radiation stress is a diagonal stress tensor for normally incident acoustic waves and the principal stretches coincide with the coordinates, so that the constitutive relation of the acoustomechanical soft

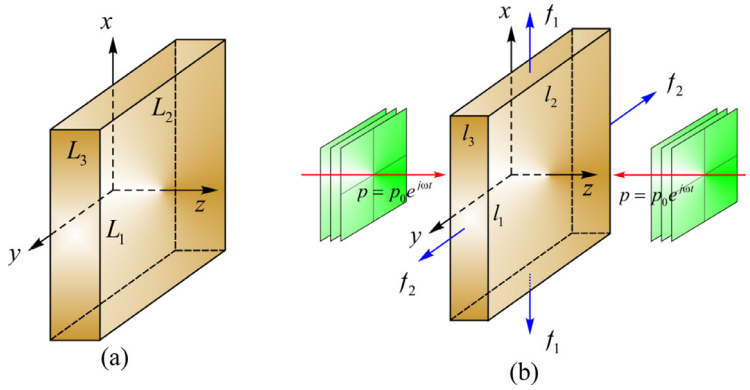

Fig. 1. Schematic illustration of a layer of soft material subjected to combined mechanical force f and two counterpropagating acoustic inputs $p = p_0 e^{j\omega t}$: (a) the layer has undeformed dimensions (L_1, L_2, L_3) in the reference configuration; (b) the layer is deformed to dimensions (l_1, l_2, l_3) in the current configuration.

material can be rewritten as:

$$\sigma_1 - \sigma_3 = \lambda_1 \frac{\partial W(\lambda_1, \lambda_2)}{\partial \lambda_1} - (\langle T_{11} \rangle - \langle T_{33} \rangle) \tag{5}$$

$$\sigma_2 - \sigma_3 = \lambda_2 \frac{\partial W(\lambda_1, \lambda_2)}{\partial \lambda_2} - (\langle T_{22} \rangle - \langle T_{33} \rangle) \tag{6}$$

The nonlinear elasticity of soft materials can be described by adopting the Gent model (Gent, 1996). In the Gent model, the Helmholtz free energy is expressed as a function of the principal stretches:

$$W(\mathbf{F}) = -\frac{\mu J_m}{2} \ln\left(1 - \frac{\lambda_1^2 + \lambda_2^2 + \lambda_3^2 - 3}{J_m}\right) \tag{7}$$

where μ is the initial shear modulus and J_m is the extension limit. The Gent model degrades to the neo-Hookean model when J_m approaches infinity. Inserting the Gent model into the constitutive relation, one obtains:

$$\sigma_1 + (t_1 - t_3) = \frac{\mu\left(\lambda_1^2 - \lambda_3^2\right)}{1 - \left(\lambda_1^2 + \lambda_2^2 + \lambda_3^2 - 3\right)/J_m} \tag{8}$$

$$\sigma_2 + (t_2 - t_3) = \frac{\mu\left(\lambda_2^2 - \lambda_3^2\right)}{1 - \left(\lambda_1^2 + \lambda_2^2 + \lambda_3^2 - 3\right)/J_m} \tag{9}$$

where the homogenized acoustic stresses along the thickness direction are given by:

$$t_1 = \frac{1}{l_3}\int_0^{l_3} \langle T_{11}(z) \rangle dz, \quad t_2 = \frac{1}{l_3}\int_0^{l_3} \langle T_{22}(z) \rangle dz,$$
$$t_3 = \left\langle T_{33}^{in}(l_3) \right\rangle - \left\langle T_{33}^{out}(l_3) \right\rangle \tag{10}$$

For a thin material layer, this spatial averaging can simplify the theoretical calculation without significant loss of the nature and the accuracy of the problem. Due to material mismatch at the interface, the acoustic radiation stress jumps discontinuously from one side $\langle T_{33}^{in}(l_3) \rangle$ to the other side $\langle T_{33}^{out}(l_3) \rangle$, the difference $t_3 = \langle T_{33}^{in}(l_3) \rangle - \langle T_{33}^{out}(l_3) \rangle$ being the resultant stress that causes material deformation.

Cauchy stresses induced by external mechanical forces f_1 and f_2 can be expressed as:

$$\sigma_1 = \frac{f_1}{l_2 l_3} = \frac{1}{\lambda_2 \lambda_3}\frac{f_1}{L_2 L_3}, \quad \sigma_2 = \frac{f_2}{l_1 l_3} = \frac{1}{\lambda_1 \lambda_3}\frac{f_2}{L_1 L_3} \tag{11}$$

Substitution of (11) into (8) and (9) yields:

$$\frac{1}{\lambda_2 \lambda_3}\frac{f_1}{L_2 L_3} + (t_1 - t_3) = \frac{\mu\left(\lambda_1^2 - \lambda_3^2\right)}{1 - \left(\lambda_1^2 + \lambda_2^2 + \lambda_3^2 - 3\right)/J_m} \tag{12}$$

$$\frac{1}{\lambda_1 \lambda_3}\frac{f_2}{L_1 L_3} + (t_2 - t_3) = \frac{\mu\left(\lambda_2^2 - \lambda_3^2\right)}{1 - \left(\lambda_1^2 + \lambda_2^2 + \lambda_3^2 - 3\right)/J_m} \tag{13}$$

Eqs. (12) and (13) can be used to characterize the nonlinear large deformation of soft materials actuated by acoustic wave at prescribed force/displacement boundary conditions. The acoustic field is solved in Eulerian coordinates, which highly depends on material deformation. Specifically, at given material configuration and acoustic inputs, both the acoustic field and the acoustic stress generated by the acoustic field are calculated. This acoustic stress causes material deformation. In turn, the deformed material configuration reshapes the acoustic field and acoustic stress distribution. Such acoustomechanical coupling reaches a steady state until the acoustic stress and mechanical stress together balance with the elastic deformation stress.

In the sections to follow, the effect of force/displacement condition on the steady-state acoustical actuation response of a thin soft material layer immersed in fluid is quantified, including equal-biaxial force, uniaxial force and uniaxial constraint.

3. Model validation

To verify the proposed acoustomechanical theory for soft materials, a numerical model is developed by using the commercially available FE (finite-element) software COMSOL Multiphysics. Since this problem includes acoustic wave propagation and material deformation, the Pressure Acoustics module and the Solid Mechanics module are adopted to establish the numerical model. The boundary conditions of wave propagation and mechanical deformation are fully taken into consideration. The length of each element is selected to be one-twenty of the acoustic wavelength at the highest frequency (10 MHz) of interest to ensure the accuracy of the numerical model.

The comparison between the proposed acoustomechanical theory and the developed FE model for the acoustomechanical response and the equivalent acoustic stresses of/on the soft material layer are presented in Fig. 2(a) and (b), respectively. As shown in Fig. 2(b), the theory agrees well with the FE model for the equivalent acoustic stresses. This is because at the given configuration of the material layer (i.e., the given thickness of the layer l_3), the acoustic fields and acoustic radiation stresses can be readily calculated without overly depending on the material deformation. However, the FE calculation of the acoustomechanical response of the soft material layer is relatively difficult. In the FE model, the material deformation and acoustic fields are strongly coupled, and thus this boundary-value problem should be dealt with by applying an incremental iterative scheme. We increased the acous-

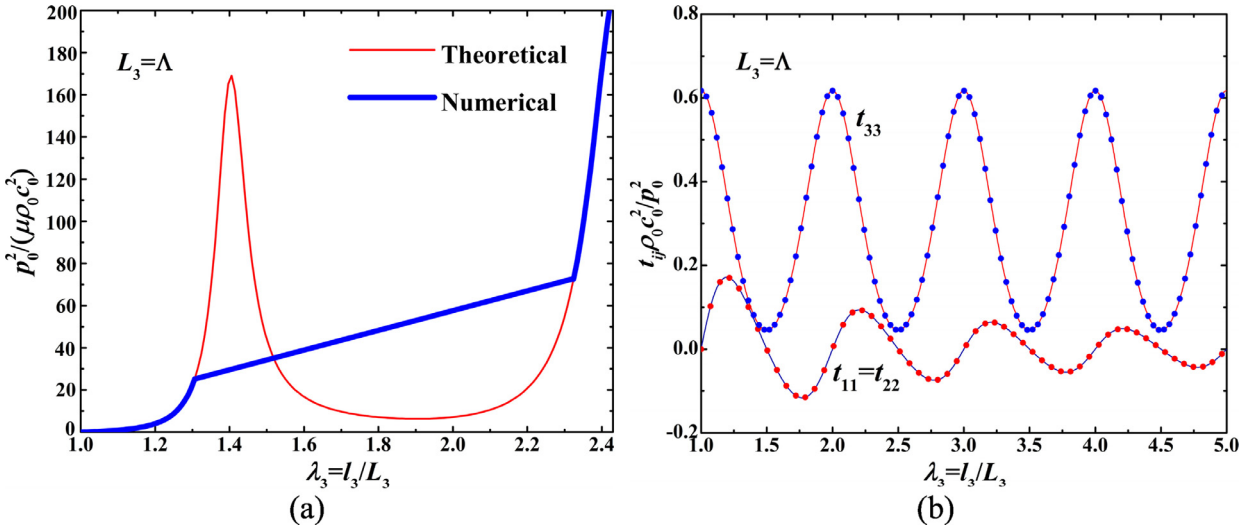

Fig. 2. (a) Comparison between the proposed theory and the numerical model. (a) the acoustomechanical response of soft material under two counterpropagating acoustic inputs; (b) the corresponding equivalent acoustic stress (solid line: theoretical results; dot: numerical results). The initial thickness of the layer is considered to be $L_3 = \Lambda$, here Λ is the acoustic wavelength in the material.

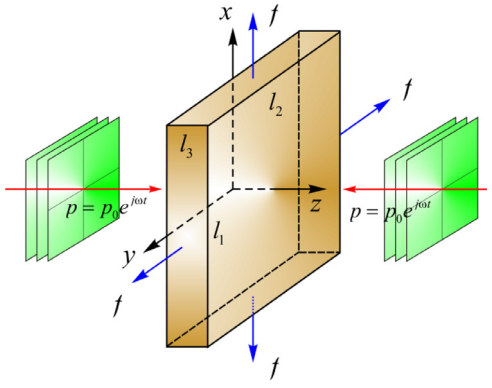

Fig. 3. A thin layer of soft material subjected to equal-biaxial force f and acoustic input $p = p_0 e^{j\omega t}$.

tic inputs $p_0^2/(\mu\rho_0 c_0^2)$ step by step, and for each increment, the FE model correspondingly calculated the acoustic radiation stress and material deformation, and then updated the acoustic fields. Repeating the above procedures, we can reach the series of steady states at which the generated acoustic radiation stress balances the deformation stress. Fig. 2(a) just plots these series of steady states, namely, the given acoustic inputs $p_0^2/(\mu\rho_0 c_0^2)$ are related to the corresponding material deformation $\lambda_3 = l_3/L_3$. The proposed acoustomechanical theory is able to give excellent predictions, while the FE model can only reproduce parts of the acoustomechanical response due to the convergence problem of numerical calculation. Of course, the FE model can be further refined if one can take more efforts to overcome the convergence problem.

4. Acoustical actuation under equal-biaxial force

Consider the acoustical actuation of a thin soft material layer subjected to equal-biaxial mechanical force, as shown in Fig. 3. The layer has undeformed dimensions (L_1, L_2, L_3) in the reference configuration. Upon exerting the equal-biaxial mechanical force f, the layer is deformed to dimensions ($\lambda^{pre}L_1$, $\lambda^{pre}L_2$, $(\lambda^{pre})^{-2}L_3$) in the prestretch configuration. Further, when acoustic inputs $p = p_0 e^{j\omega t}$ are applied through the layer thickness, the two counterpropagating acoustic waves generate a symmetric acoustic field as well as symmetric distribution of acoustic stress along the thickness direction. Hence, one has $\lambda_1 = \lambda_2 = \lambda$ and $\lambda_3 = \lambda^{-2}$due to material deformation, with mechanical stresses $\sigma_1 = \sigma_2 = \lambda f/(L_2 L_3)$and acoustic stresses $t_1 = \frac{1}{l_3}\int_0^{l_3}\langle T_{11}(z)\rangle dz$ and $t_3 = \langle T_{33}^{in}(l_3)\rangle - \langle T_{33}^{out}(l_3)\rangle$ generated in the current actuated configuration. Accordingly, the constitutive equations of (12) and (13) degrade to

$$\frac{\lambda f}{L_2 L_3} + (t_1 - t_3) = \frac{\mu(\lambda^2 - \lambda^{-4})}{1 - (2\lambda^2 + \lambda^{-4} - 3)/J_m} \tag{14}$$

which describes the stretch λ of the soft material layer caused by equal-biaxial force f and acoustic inputs $p = p_0 e^{j\omega t}$. At prescribed normalized mechanical force $f/(\mu L_2 L_3)$, the normalized acoustic stress is a function of material stretch λ, as

$$\frac{p_0^2}{\mu\rho_0 c_0^2} = \frac{1}{(t_1 - t_3)}\frac{p_0^2}{\rho_0 c_0^2}\left[\frac{\mu\left(\lambda^2 - \lambda^{-4}\right)}{1 - \left(2\lambda^2 + \lambda^{-4} - 3\right)/J_m} - \frac{\lambda}{\mu}\frac{f}{L_2 L_3}\right] \tag{15}$$

Correspondingly, for this fixed mechanical force $f/(\mu L_2 L_3)$, the prestretch λ^{pre} of the soft material layer can be obtained by solving the following equation

$$\frac{f}{\mu L_2 L_3} = \frac{\lambda^{pre} - (\lambda^{pre})^{-5}}{1 - \left[2(\lambda^{pre})^2 + (\lambda^{pre})^{-4} - 3\right]/J_m} \tag{16}$$

With the mechanical force $f/(\mu L_2 L_3)$ fixed, as the acoustic stress is increased, the material layer deforms to a succession of equilibrium states, as shown by the stretch-stress relation curve of Fig. 4(a). The prestretch λ^{pre} induced by the mechanical force is obtained from the initially acoustic load point, namely, the interaction between the stretch-stress curve and the zero acoustic stress line. At certain prestretch and acoustic stress, there exist at least one or multiple equilibrium states, demonstrating the nonlinear acoustomechanical behavior of the soft material layer. For different prestretches, the stretch-stress curves exhibit different trends. When the prestretch is small, the curve varies significantly with multiple peaks and dips. When the prestretch is large, the curve varies with fewer peaks and dips.

The trend of the curve can be interpreted by the variation of acoustic stress with stretch. As shown in Fig. 4(b), as the in-plane stretch increases, the initially intensive fluctuation of the acoustic

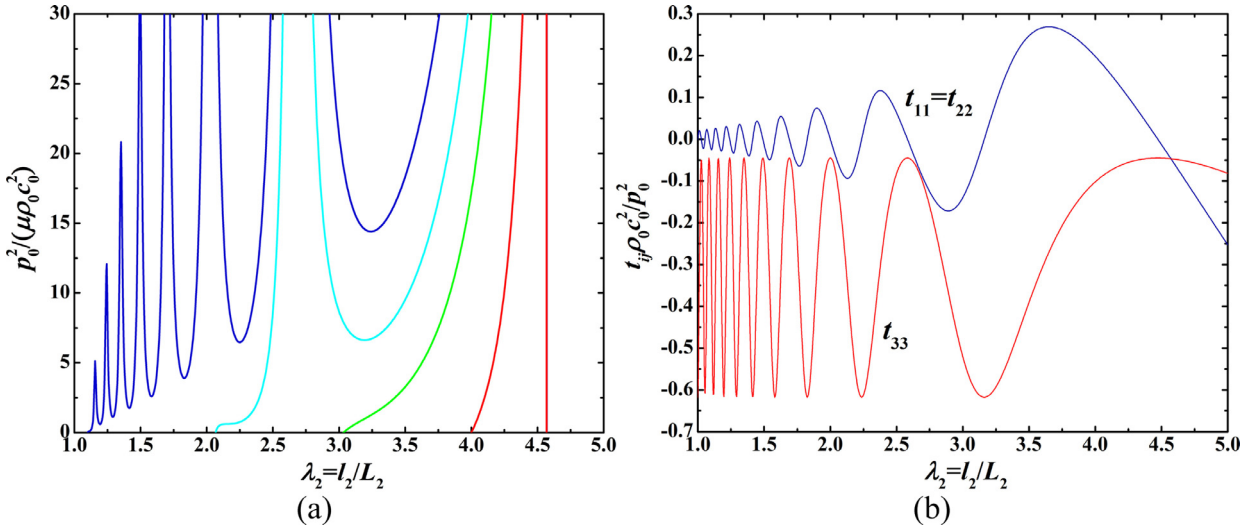

Fig. 4. (a) Acoustomechanical response of soft material under equal-biaxial mechanical force; (b) the corresponding equivalent acoustic stress. The initial thickness of the layer is considered to be $L_3/\Lambda = 10$, here Λ is the acoustic wavelength in the material.

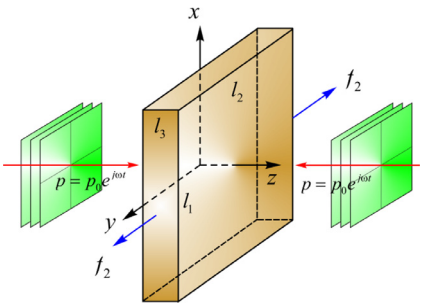

Fig. 5. A layer of soft material subjected to uniaxial force f_2 and acoustic inputs $p = p_0e^{j\omega t}$.

stress becomes less intensive, which causes the variation trend of the stretch-stress curve in Fig. 4(a). When $t_1 - t_3$ approaches zero, a peak appears in the stretch-stress curve, while a dip occurs when $t_1 - t_3$ reaches a local maximum. The fluctuation of the stretch-stress curve implies multiple snap-through instabilities: when the acoustic stress reaches local maximum, any further ramping up of the stress will induce a discontinuous jumping of material deformation to a much larger deformation. This phenomenon enables giant acoustical actuation at relatively small acoustic inputs.

5. Acoustical actuation under uniaxial force

Consider a soft material layer subjected to a uniaxial mechanical force and two counterpropagating acoustic waves, as shown in Fig. 5. In the reference configuration, the layer has undeformed dimensions (L_1, L_2, L_3). In the prestretch configuration, the layer deforms to dimensions ($(\lambda^{pre})^{-1/2}L_1$, $\lambda^{pre}L_2$, $(\lambda^{pre})^{-1/2}L_3$) when uniaxial mechanical force f_2 is applied. When acoustic inputs $p = p_0e^{j\omega t}$ are applied through layer thickness, the layer deforms to dimensions (λ_1L_1, λ_2L_2, λ_3L_3) in the actuation configuration. The principal stretches are (λ_1, λ_2, $\lambda_3 = (\lambda_1\lambda_2)^{-1}$) while the mechanical stresses are $\sigma_1 = 0$ and $\sigma_2 = \lambda_2 f/(L_1L_3)$. The acoustic stresses $t_1 = \frac{1}{l_3}\int_0^{l_3}\langle T_{11}(z)\rangle dz$ and $t_3 = \langle T_{33}^{in}(l_3)\rangle - \langle T_{33}^{out}(l_3)\rangle$ can be calculated by employing the acoustic fields in the current (actuated) configuration. Eqs. (12) and (13) thence degrade to:

$$(t_1 - t_3) = \frac{\mu\left(\lambda_1^2 - \lambda_3^2\right)}{1 - \left(\lambda_1^2 + \lambda_2^2 + \lambda_3^2 - 3\right)/J_m} \tag{17}$$

$$\frac{1}{\lambda_1\lambda_3}\frac{f_2}{L_1L_3} + (t_2 - t_3) = \frac{\mu\left(\lambda_2^2 - \lambda_3^2\right)}{1 - \left(\lambda_1^2 + \lambda_2^2 + \lambda_3^2 - 3\right)/J_m} \tag{18}$$

Deformation of the thin soft layer at equilibrium states can be obtained by solving the above two equations at given mechanical force and acoustic inputs.

When the layer is only subjected to uniaxial mechanical force, the prestretch $\lambda_2^{pre} = \lambda^{pre}(\lambda_1^{pre} = \lambda_3^{pre} = (\lambda^{pre})^{-1/2})$ is obtained by:

$$\frac{f_2}{\mu L_1L_3} = \frac{\lambda^{pre} - (\lambda^{pre})^{-2}}{1 - \left[2(\lambda^{pre})^{-1} + (\lambda^{pre})^2 - 3\right]/J_m} \tag{19}$$

In the current actuated configuration, the principal stretches λ_1 and λ_2 are related to each other by:

$$\left(1 - \frac{\lambda_2}{J_m}\frac{f_2}{\mu L_1L_3}\right)\lambda_1^4 + \left[\frac{\lambda_2}{J_m}\frac{f_2}{\mu L_1L_3}\left(J_m - \lambda_2^2 + 3\right) - \lambda_2^2\right]\lambda_1^2 - \frac{\lambda_2}{J_m}\frac{f_2}{\mu L_1L_3}\lambda_2^{-2} = 0 \tag{20}$$

Inserting Eq. (20) into Eq. (17), one obtains the normalized acoustic stress as:

$$\frac{p_0^2}{\mu\rho_0c_0^2} = \frac{1}{(t_1 - t_3)}\frac{p_0^2}{\rho_0c_0^2}\frac{\left(\lambda_1^2 - \lambda_3^2\right)}{1 - \left(\lambda_1^2 + \lambda_2^2 + \lambda_3^2 - 3\right)/J_m} \tag{21}$$

Under fixed uniaxial mechanical force $f_2/(\mu L_1L_3)$, the layer undergoes a succession of equilibrium states when the acoustic stress increases, as illustrated by the stretch-stress relation curve in Fig. 6. The prestretch is obtained directly from the interaction between the stretch-stress curve and the zero acoustic stress line. For any given mechanical force and acoustic stress, the acoustomechanical response exhibits nonlinear behavior as at least one or multiple equilibrium states exist. Similar to the equal-biaxial force case, the fluctuation trend can be explained by the variation of acoustic stress as a function of in-plane stretch. Different uniaxial prestretches lead to different acoustically triggered material deformations. Therefore, the corresponding acoustic stresses are presented in Fig. 7 for selected uniaxial prestretches. When the prestretch is small, the fluctuation of the acoustic stress is firstly intensive and then less intensive (Fig. 7(a) and (b)). When the prestretch is large, the fluctuation changes from firstly less intensive to intensive and eventually to less intensive (Fig. 7(c) and (d)).

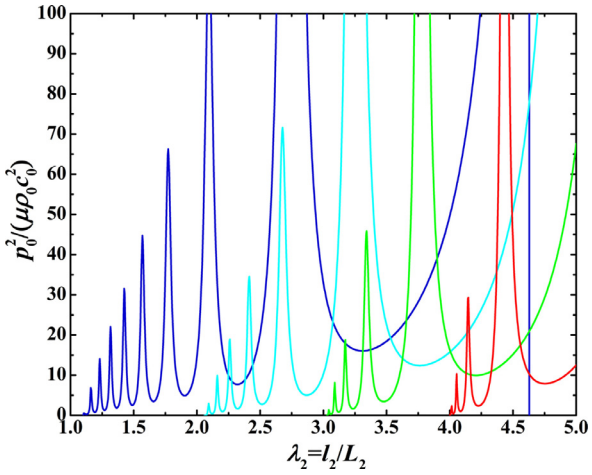

Fig. 6. Acoustomechanical response of a thin soft material layer under uniaxial mechanical force, with its initial layer thickness $L_3/\Lambda = 10$, Λ being acoustic wavelength in the material.

Such variation of the acoustic stress affects the trend of stretch-stress curve (Fig. 6), reaching maximum when $t_1 - t_3$ approaches zero and minimum when $t_1 - t_3$ approaches maximum. Such nonlinearity in acoustomechanical response of soft material offers a wide space to design novel acoustic actuators.

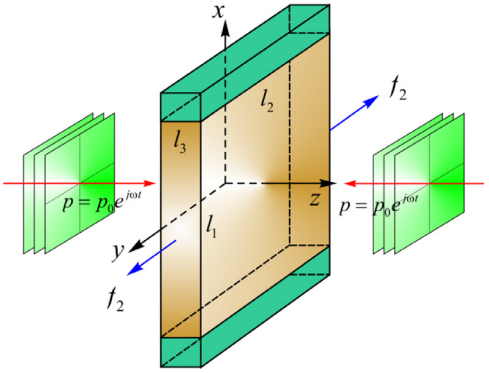

Fig. 8. A thin layer of soft material constrained in x-direction and subjected to mechanical force f_2 and acoustic inputs $p = p_0e^{j\omega t}$.

6. Acoustical actuation under uniaxial constraint

With reference to Fig. 8, consider a thin soft material layer subjected to uniaxial constraint in the x-direction and uniaxial mechanical force f_2 in the y-direction. Two opposing acoustic waves impinge upon the layer along its thickness direction. In the ref-

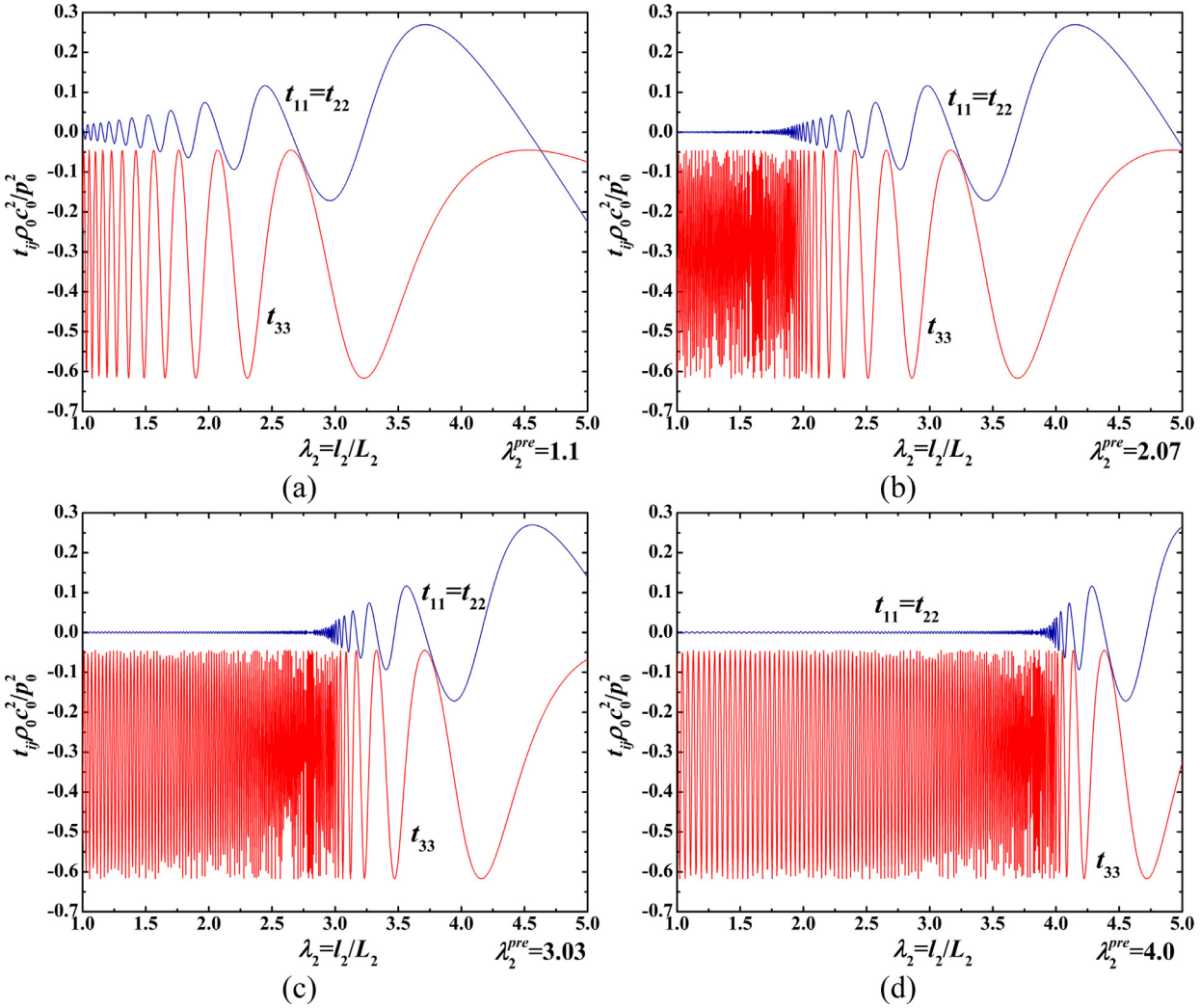

Fig. 7. Equivalent acoustic stress of a thin soft material layer under uniaxial force at selected values of prestrecth λ_2^{pre}, with its initial layer thickness $L_3/\Lambda = 10$: (a) $\lambda_2^{pre} = 1.1$; (b) $\lambda_2^{pre} = 2.07$; (c) $\lambda_2^{pre} = 3.03$; (d) $\lambda_2^{pre} = 4.0$.

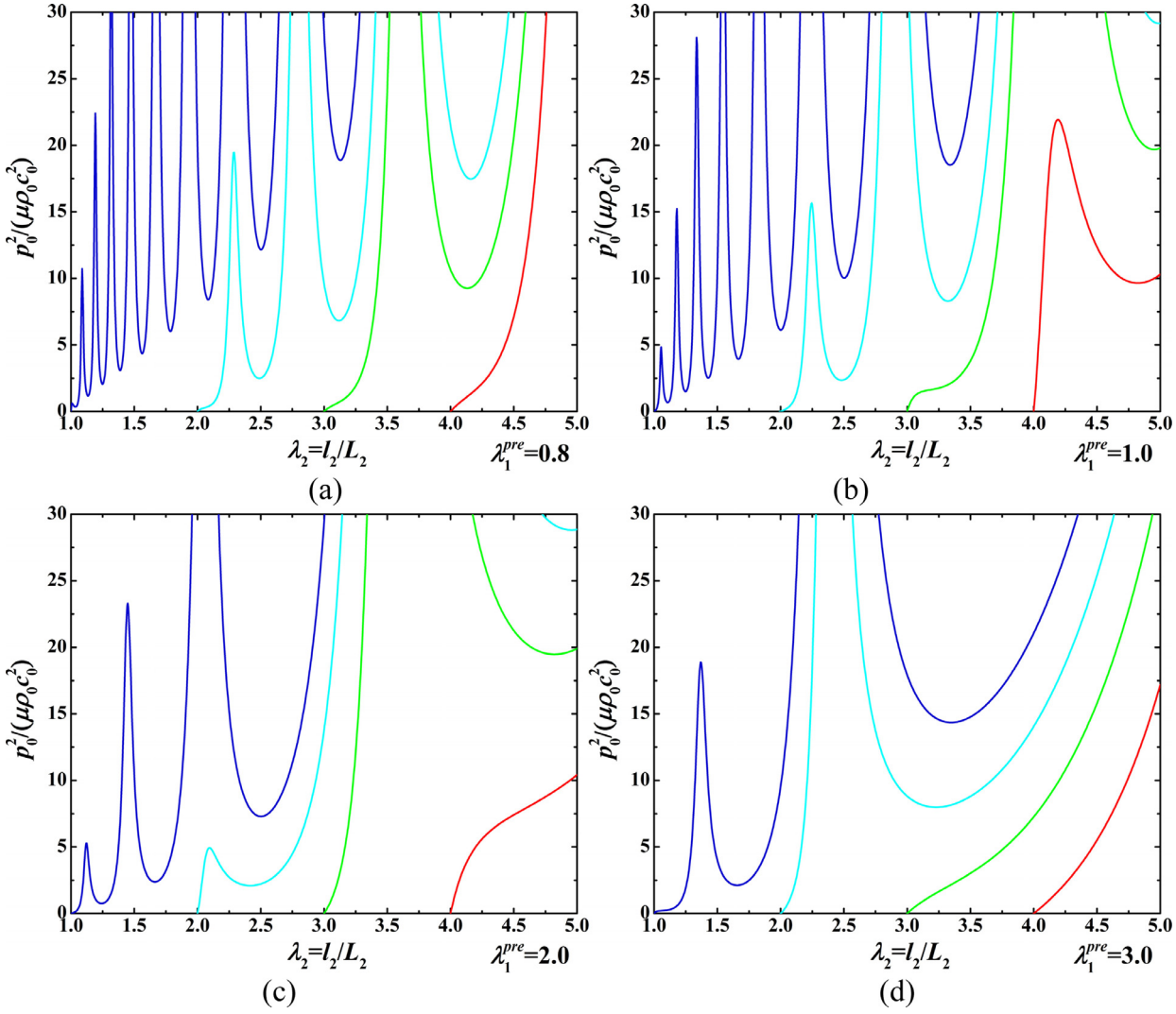

Fig. 9. Acoustomechanical response of a thin soft material layer under uniaxial constraint condition at selected prestretches: (a) $\lambda_1^{pre} = 0.8$; (b) $\lambda_1^{pre} = 1.0$; (c) $\lambda_1^{pre} = 2.0$; (d) $\lambda_1^{pre} = 3.0$. The layer has an initial thickness of $L_3/\Lambda = 10$, Λ being acoustic wavelength in the material.

erence configuration, the layer has undeformed dimensions (L_1, L_2, L_3). In the prestretch configuration, the layer is uniaxially stretched to have a stretch λ_1^{pre} and then fixed onto a rigid substrate in the x-direction. Thereafter, the layer with prestretch λ_2^{pre} is uniaxially stretched by mechanical force f_2 in the y-direction. In the current actuated configuration, the layer is deformed to have principal stretches (λ_1, λ_2, λ_3) when acoustic inputs $p = p_0 e^{j\omega t}$ are applied through its thickness. Clearly, the mechanical stresses $\sigma_1 \neq 0$ and $\sigma_2 = \lambda_2 f_2/(L_1L_3)$. The acoustic stresses $t_1 = \frac{1}{l_3}\int_0^{l_3}\langle T_{11}(z)\rangle dz$ and $t_3 = \langle T_{33}^{in}(l_3)\rangle - \langle T_{33}^{out}(l_3)\rangle$ are calculated using the acoustic fields in the current actuated configuration. Therefore, Eqs. (12) and (13) become

$$\sigma_1 + (t_1 - t_3) = \frac{\mu\left(\lambda_1^2 - \lambda_3^2\right)}{1 - \left(\lambda_1^2 + \lambda_2^2 + \lambda_3^2 - 3\right)/J_m} \tag{22}$$

$$\frac{\lambda_2 f_2}{L_1L_3} + (t_2 - t_3) = \frac{\mu\left(\lambda_2^2 - \lambda_3^2\right)}{1 - \left(\lambda_1^2 + \lambda_2^2 + \lambda_3^2 - 3\right)/J_m} \tag{23}$$

In the process of acoustically actuated deformation, given the mechanical force $\lambda_2 f_2/(L_1L_3)$ and acoustic inputs, the stretch λ_2 of the thin layer is determined by (23) and the constraint stress σ_1 is determined by (22).

Given the prestretch λ_1^{pre} and the mechanical force $f_2/(\mu L_1L_3)$, the layer endures another prestretch λ_2^{pre} that can be calculated by:

$$\frac{f_2}{\mu L_1L_3} = \frac{\lambda_2^{pre} - \left(\lambda_1^{pre}\right)^{-2}\left(\lambda_2^{pre}\right)^{-3}}{1 - \left[\left(\lambda_1^{pre}\right)^2 + \left(\lambda_2^{pre}\right)^2 + \left(\lambda_1^{pre}\lambda_2^{pre}\right)^{-2} - 3\right]/J_m} \tag{24}$$

Substitution of Eq. (24) into (23) leads to the normalized acoustic stress:

$$\frac{p_0^2}{\mu\rho_0c_0^2} = \frac{1}{(t_2 - t_3)}\frac{p_0^2}{\rho_0c_0^2}\left[\frac{\left(\lambda_2^2 - \lambda_3^2\right)}{1 - \left(\lambda_1^2 + \lambda_2^2 + \lambda_3^2 - 3\right)/J_m} - \frac{\lambda_2}{\mu}\frac{f_2}{L_1L_3}\right] \tag{25}$$

To investigate the acoustomechanical response of the thin layer under uniaxial constraint and uniaxial mechanical force condition, four prestretches ($\lambda_1^{pre} = 0.8$, 1, 2 and 3) are selected as shown in Fig. 9. As the acoustic stress increases, a succession of equilibrium states are achieved in the layer, as evidenced by the stretch-stress relation curves of Fig. 9. The value of λ_2^{pre} is read from the interaction between the stretch-stress curve and the zero acoustic stress line. The fluctuation of the stretch-stress curve demonstrates the nonlinear acoustomechanical response of the layer, which is

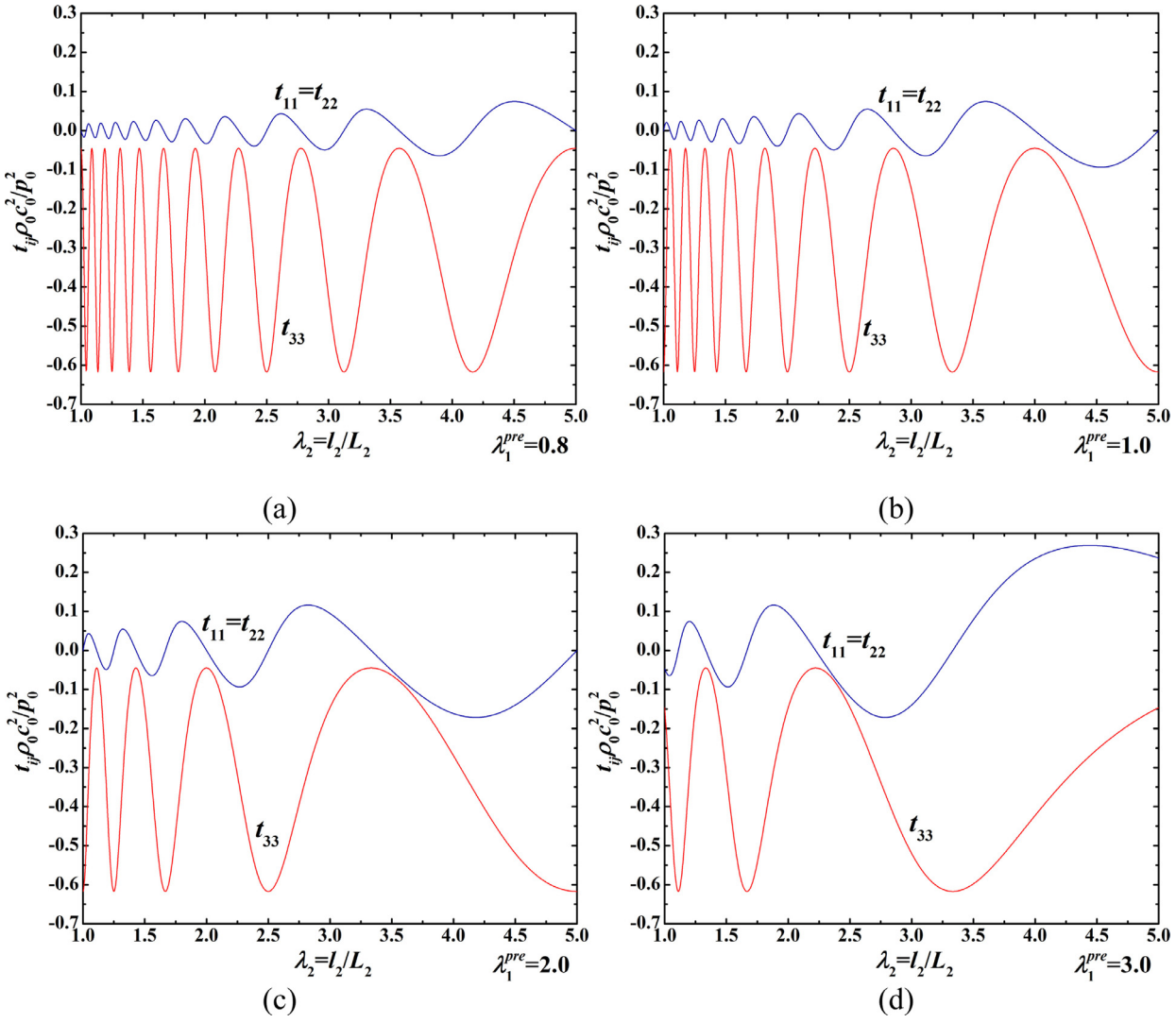

Fig. 10. Equivalent acoustic stress of a thin soft material layer ($L_3/\Lambda = 10$) under uniaxial constraint condition at selected prestretches: (a) $\lambda_1^{pre} = 0.8$; (b) $\lambda_1^{pre} = 1.0$; (c) $\lambda_1^{pre} = 2.0$; (d) $\lambda_1^{pre} = 3.0$.

directly related to the variation of acoustic stress with increasing in-plane stretch (Fig. 10). The fluctuation of the acoustic stress is firstly less intensive and then intensive, resulting in the variation trend of stretch-stress curve in Fig. 9. The intensive fluctuation whenλ_2^{pre} is small becomes less intensive when λ_2^{pre} becomes large. To maintain the deformation, the required acoustic stress reaches maximum when $t_1 - t_3$ approaches zero and minimum when $t_1 - t_3$ approaches its maximum. The significant effect of prestretch can be used to enhance acoustically actuated material deformation.

7. Concluding remarks

We develop an acoustomechanical theory for soft materials subjected to simultaneous mechanical forces and acoustic radiation forces by combining the nonlinear elasticity theory of soft materials with the acoustic radiation stress theory. For illustration, two counterpropagating ultrasonic waves impinging onto the surfaces of a thin soft material layer immersed in fluid is considered. The resulting acoustic field is capable of giving rise to acoustic radiation stress in and out of the thin layer, particularly at the interface between the soft material and the surrounding medium. While the acoustic radiation stress deforms the material, the deformed configuration of the soft material in turn is able to reconstruct the acoustic field and the distribution of the acoustic radiation stress. The material reaches a steady deformation state when the mechanical stress and acoustic stress balance with the material deformation stress.

The developed theory is employed to investigate the sequence of equilibrium state and the acoustomechanical response of thin soft material layer under three different force/displacement boundary conditions: equal-biaxial force, uniaxial force and uniaxial constraint. The results demonstrate the significant influence of boundary condition on acoustomechanical response. Further, as wave propagation is sensitive to material configuration, prestretching the soft material affects remarkably the acoustomechanical behavior. Specifically, when the thin soft material layer is acoustically triggered from different prestretches, it shows different stretch versus stress relations, useful for designing novel acoustic sensors and actuators.

Acknowledgements

This work was supported by the National Natural Science Foundation of China (51528501) and the Fundamental Research Funds for Central Universities (2014qngz12).

Appendix. Acoustic fields of two counterpropagating waves

Although a real acoustic wave propagates through a soft material at nonlinear level, the calculation of the induced acoustic radiation stress only needs a linear level analysis for the acoustic fields. Because the acoustic radiation stress scales as the second-order of the acoustic fields, it can be expressed using the first-order terms, i.e., the linear acoustic pressure and the linear velocity. Therefore, in this appendix, acoustic wave propagation at linear level is analyzed by rigorously considering boundary conditions.

Acoustic wave propagation in medium is governed by the Helmholtz equation $\Delta\phi - \frac{1}{c_a^2}\frac{\partial^2\phi}{\partial t^2} = 0$, ϕ being the acoustic velocity potential and $c_a = (\partial p/\partial\rho)_s$ the acoustic speed. Generally, the acoustic impedance of the soft material mismatches with that of the outside surrounding medium so that $\rho_1 c_1 \neq \rho_2 c_2$. The acoustic field in each medium consists of both positive-going and negative-going waves. As illustrated in Fig. 1(b), the acoustic boundary conditions need to ensure the continuity of acoustic pressure and velocity at the interfaces:

$$p_1 = p_2|_{z=0}, \quad p_2 = p_3|_{z=l_3}, \tag{A1}$$

$$u_{1z} = u_{2z}|_{z=0}, \quad u_{2z} = u_{3z}|_{z=l_3}, \tag{A2}$$

where (p_1, p_2, p_3) are the acoustic pressures and (u_{1z}, u_{2z}, u_{3z}) are the components of the velocity along the z-direction in the left medium, soft material and the right medium, respectively.

Obeying the governing equation of wave propagation and the boundary conditions of (A1) and (A2), the acoustic fields generated by two counterpropagating acoustic waves are the superposition of these two opposing fields, as:

$$p^{in} = \frac{2\omega I\rho_1\rho_2 k_{1z} e^{j\omega t}[\rho_2 k_{1z}\sin(k_{2z}(z-l_3)) - \rho_2 k_{1z}\sin(k_{2z}z) + j\rho_1 k_{2z}\cos(k_{2z}(z-l_3)) + j\rho_1 k_{2z}\cos(k_{2z}z)]}{2\rho_1\rho_2 k_{1z}k_{2z}\cos(k_{2z}l_3) + j\left(\rho_1^2 k_{2z}^2 + \rho_2^2 k_{1z}^2\right)\sin(k_{2z}l_3)} \tag{A3}$$

$$u^{in} = \frac{2I\rho_1 k_{1z}k_{2z} e^{j\omega t}[\rho_1 k_{2z}\sin(k_{2z}(z-l_3)) + \rho_1 k_{2z}\sin(k_{2z}z) + j\rho_2 k_{1z}\cos(k_{2z}(z-l_3)) - j\rho_2 k_{1z}\cos(k_{2z}z)]}{2\rho_1\rho_2 k_{1z}k_{2z}\cos(k_{2z}l_3) + j\left(\rho_1^2 k_{2z}^2 + \rho_2^2 k_{1z}^2\right)\sin(k_{2z}l_3)} \tag{A4}$$

$$p_R^{out} = j\omega\rho_3 I e^{j\omega t}\left[e^{jk_{3z}(z-l_3)} + e^{-jk_{3z}(z-l_3)}\frac{j\sin(k_{2z}l_3)\left(\rho_2^2 k_{1z}^2 - \rho_1^2 k_{2z}^2\right) + 2\rho_1\rho_2 k_{1z}k_{2z}}{2\rho_1\rho_2 k_{1z}k_{2z}\cos(k_{2z}l_3) + j\left(\rho_1^2 k_{2z}^2 + \rho_2^2 k_{1z}^2\right)\sin(k_{2z}l_3)}\right] \tag{A5}$$

$$u_R^{out} = jk_{3z} I e^{j\omega t}\left(-e^{jk_{3z}(z-l_3)} + e^{-jk_{3z}(z-l_3)}\frac{j\sin(k_{2z}l_3)\left(\rho_2^2 k_{1z}^2 - \rho_1^2 k_{2z}^2\right) + 2I\rho_1\rho_2 k_{1z}k_{2z}}{2\rho_1\rho_2 k_{1z}k_{2z}\cos(k_{2z}l_3) + j\left(\rho_1^2 k_{2z}^2 + \rho_2^2 k_{1z}^2\right)\sin(k_{2z}l_3)}\right) \tag{A6}$$

where p and u are the acoustic pressure field and velocity field, respectively. The superscripts "in/out" represent the corresponding variables related to the inside and outside media, respectively. The subscripts 1, 2 and 3 denote the left medium, the soft material and the right medium, respectively. ω is the angular frequency, I is the amplitude of incident velocity potential, ρ is the medium density, and k is the acoustic wavenumber.

Under such conditions, the acoustic radiation stresses are:

$$\left\langle T_{11}^{in}\right\rangle = \left\langle T_{22}^{in}\right\rangle = \frac{\tau_2\varsigma_2^* e^{-2jk_{2z}z} + \tau_2^*\varsigma_2 e^{2jk_{2z}z}}{2\rho_2 c_2^2}, \left\langle T_{33}^{in}\right\rangle = \frac{\tau_2\tau_2^* + \varsigma_2\varsigma_2^*}{2\rho_2 c_2^2} \tag{A7}$$

$$\left\langle T_{11}^{out}\right\rangle = \left\langle T_{22}^{out}\right\rangle = \frac{\tau_1\varsigma_1^* e^{-2jk_{2z}z} + \tau_1^*\varsigma_1 e^{2jk_{2z}z}}{2\rho_1 c_1^2}, \left\langle T_{33}^{out}\right\rangle = \frac{\tau_1\tau_1^* + \varsigma_1\varsigma_1^*}{2\rho_1 c_1^2}, \tag{A8}$$

The equivalent stresses are:

$$t_1 = t_2 = \frac{1}{2\rho_2 c_2^2}\left\{\frac{1}{2jk_{2z}l_3}[\tau_2^*\varsigma_2(e^{2jk_{2z}l_3} - 1) - \tau_2\varsigma_2^*(e^{-2jk_{2z}l_3} - 1)]\right\} \tag{A9}$$

$$t_3 = \frac{\tau_2\tau_2^* + \varsigma_2\varsigma_2^*}{2\rho_2 c_2^2} - \frac{\tau_1\tau_1^* + \varsigma_1\varsigma_1^*}{2\rho_1 c_1^2} \tag{A10}$$

where the superscript asterisk * means the complex conjugate of the corresponding variable, and we have

$$\tau_1 = j\omega\rho_1 I e^{jk_{1z}l_3} \times\left(\frac{j\left(\rho_2^2 k_{1z}^2 - \rho_1^2 k_{2z}^2\right)\sin(k_{2z}l_3) + 2\rho_1\rho_2 k_{1z}k_{2z}}{2\rho_1\rho_2 k_{1z}k_{2z}\cos(k_{2z}l_3) + j\left(\rho_1^2 k_{2z}^2 + \rho_2^2 k_{1z}^2\right)\sin(k_{2z}l_3)}\right) \tag{A11}$$

$$\tau_2 = j\omega\rho_1\rho_2 k_{1z} I \times\left(\frac{e^{jk_{2z}l_3}(\rho_2 k_{1z} + \rho_1 k_{2z}) + (\rho_1 k_{2z} - \rho_2 k_{1z})}{2\rho_1\rho_2 k_{1z}k_{2z}\cos(k_{2z}l_3) + j\left(\rho_1^2 k_{2z}^2 + \rho_2^2 k_{1z}^2\right)\sin(k_{2z}l_3)}\right) \tag{A12}$$

$$\varsigma_1 = j\omega\rho_1 I e^{-jk_{1z}l_3} \tag{A13}$$

$$\varsigma_2 = j\omega\rho_1\rho_2 k_{1z} I \times\left(\frac{e^{-jk_{2z}l_3}(\rho_1 k_{2z} - \rho_2 k_{1z}) + (\rho_2 k_{1z} + \rho_1 k_{2z})}{2\rho_1\rho_2 k_{1z}k_{2z}\cos(k_{2z}l_3) + j\left(\rho_1^2 k_{2z}^2 + \rho_2^2 k_{1z}^2\right)\sin(k_{2z}l_3)}\right) \tag{A14}$$

References

Beyer, R.T., 1978. Radiation pressure-the history of a mislabeled tensor. J. Acoust. Soc. Am. 63, 1025–1030.

Borgnis, F.E., 1953. Acoustic radiation pressure of plane compressional waves. Rev. Modern Phys. 25, 653–664.

Brandt, E.H., 2001. Acoustic physics: suspended by sound. Nature 413, 474–475.

Brillouin, L., 1925. Ann. Phys. (Paris) 4, 528.

Bustamante, R., Dorfmann, A., Ogden, R., 2006. Universal relations in isotropic nonlinear magnetoelasticity. Quart. J. Mech. Appl. Math. 59, 435–450.

Caleap, M., Drinkwater, B.W., 2014. Acoustically trapped colloidal crystals that are reconfigurable in real time. Proc. Natl. Acad. Sci. 111, 6226–6230.

Chester, S.A., Anand, L., 2011. A thermo-mechanically coupled theory for fluid permeation in elastomeric materials: application to thermally responsive gels. J. Mech. Phys. Solids. 59, 1978–2006.

Doinikov, A.A., 1994. Acoustic radiation pressure on a rigid sphere in a viscous fluid. P. Roy. Soc. A 447, 447–466.

Dorfmann, A., Ogden, R.W., 2004. Nonlinear magnetoelastic deformations. Q. J. Mech. Appl. Math. 57, 599–622.

Evander, M., Nilsson, J., 2012. Acoustofluidics 20: applications in acoustic trapping. Lab Chip 12, 4667–4676.

Foresti, D., Nabavi, M., Klingauf, M., Ferrari, A., Poulikakos, D., 2013. Acoustophoretic contactless transport and handling of matter in air. Proc. Natl. Acad. Sci. 110, 12549–12554.

Foresti, D., Poulikakos, D., 2014. Acoustophoretic contactless elevation, orbital transport and spinning of matter in air. Phys. Rev. Lett. 112, 024301.
Gent, A.N., 1996. A new constitutive relation for rubber. Rubber Chem. Technol. 69, 59–61.
Guo, F., Mao, Z., Chen, Y., Xie, Z., Lata, J.P., Li, P., Ren, L., Liu, J., Yang, J., Dao, M., Suresh, S., Huang, T.J., 2016. Three-dimensional manipulation of single cells using surface acoustic waves. Proc. Natl. Acad. Sci. 113, 1522–1527.
Hasegawa, T., Yosioka, K., 1969. Acoustic-radiation force on a solid elastic sphere. J. Acoust. Soc. Am. 46, 1139–1143.
Hu, J.H., Ong, L.B., Yeo, C.H., Liu, Y.Y., 2007. Trapping, transportation and separation of small particles by an acoustic needle. Sens. Actuat. A 138, 187–193.
Huebsch, N., Kearney, C.J., Zhao, X., Kim, J., Cezar, C.A., Suo, Z., Mooney, D.J., 2014. Ultrasound-triggered disruption and self-healing of reversibly cross-linked hydrogels for drug delivery and enhanced chemotherapy. Proc. Natl. Acad. Sci. 111, 9762–9767.
Issenmann, B., Nicolas, A., Wunenburger, R., Manneville, S., Delville, J.P., 2008. Deformation of acoustically transparent fluid interfaces by the acoustic radiation pressure. EPL 83, 34002.
King, L.V., 1934. On the acoustic radiation pressure on spheres. P. Roy. Soc. A 147, 212–240.
Lee, C.P., Wang, T.G., 1993. Acoustic radiation pressure. J. Acoust. Soc. Am. 94, 1099–1109.
Livett, A.J., Emery, E.W., Leeman, S., 1981. Acoustic radiation pressure. J. Sound Vib. 76, 1–11.
Marx, V., 2015. Biophysics: using sound to move cells. Nat. Meth. 12, 41–44.
Mishra, P., Hill, M., Glynne-Jones, P., 2014. Deformation of red blood cells using acoustic radiation forces. Biomicrofluidics 8, 034109.
Ohmine, I., Tanaka, T., 1982. Salt effects on the phase transition of ionic gels. J. Chem. Phys. 77, 5725–5729.
Rayleigh, L., 1902. On the pressure of vibrations. Philo. Mag. 3, 338–346.
Rayleigh, L., 1905. On the momentum and pressure of gaseous vibrations, and on the connexion with the virial theorem. Philo. Mag. Ser. 6 10, 364–374.
Rudykh, S., Bertoldi, K., 2013. Stability of anisotropic magnetorheological elastomers in finite deformations: a micromechanical approach. J. Mech. Phys. Solids. 61, 949–967.
Shi, J., Ahmed, D., Mao, X., Lin, S.-C.S., Lawit, A., Huang, T.J., 2009. Acoustic tweezers: patterning cells and microparticles using standing surface acoustic waves (SSAW). Lab Chip 9, 2890–2895.
Silva, G.T., Baggio, A.L., 2015. Designing single-beam multitrapping acoustical tweezers. Ultrasonics 56, 449–455.
Stark, K.H., Garton, C.G., 1955. Electric strength of irradiated polythene. Nature 176, 1225–1226.
Suo, Z., Zhao, X., Greene, W.H., 2008. A nonlinear field theory of deformable dielectrics. J. Mech. Phys. Solids. 56, 467–486.
Tanaka, T., Fillmore, D., Sun, S.T., Nishio, I., Swislow, G., Shah, A., 1980. Phase transitions in ionic gels. Phys. Rev. Lett. 45, 1636–1639.
Walker, W.F., 1999. Internal deformation of a uniform elastic solid by acoustic radiation force. J. Acoust. Soc. Am. 105, 2508–2518.
Xie, W.J., Cao, C.D., Lü, Y.J., Wei, B., 2002. Levitation of iridium and liquid mercury by ultrasound. Phys. Rev. Lett. 89, 104304.
Xin, F., Lu, T., 2016a. Acoustomechanics of semicrystalline polymers. Theore. Appl. Mech. Lett. 6, 38–41.
Xin, F.X., Lu, T.J., 2016b. Acoustomechanical constitutive theory of soft materials. Acta Mech. Sin. 32, 828–840.
Xin, F.X., Lu, T.J., 2016c. Acoustomechanical giant deformation of soft elastomers with interpenetrating networks. Smart Mater. Strtuct. 25, 07LT02.
Xin, F.X., Lu, T.J., 2016d. Generalized method to analyze acoustomechanical stability of soft materials. J. Appl. Mech. 83, 071004.
Xin, F.X., Lu, T.J., 2016e. Tensional acoustomechanical soft metamaterials. Scientific Reports 6, 27432.
Yeh, P.D., Alexeev, A., 2015. Mesoscale modelling of environmentally responsive hydrogels: emerging applications. Chem. Commun. 51, 10083–10095.
Yosioka, K., Kawasima, Y., 1955. Acoustic radiation pressure on a compressible sphere. Acta. Acust. Acust. 5, 167–173.
Zhang, Q.M., Bharti, V., Zhao, X., 1998. Giant electrostriction and relaxor ferroelectric behavior in electron-irradiated poly(vinylidene fluoride-trifluoroethylene) copolymer. Science 280, 2101–2104.
Zhang, Q.M., Li, H., Poh, M., Xia, F., Cheng, Z.Y., Xu, H., Huang, C., 2002. An all-organic composite actuator material with a high dielectric constant. Nature 419, 284–287.
Zhao, X., Wang, Q., 2014. Harnessing large deformation and instabilities of soft dielectrics: theory, experiment, and application. Appl. Phys. Rev. 1, 021304.